Producing and controlling half-cycle near-infrared electric-field transients

Hammond, T. J.; Villeneuve, D. M.; Corkum, P. B.

Publisher's version / Version de l'éditeur:
https://doi.org/10.1364/OPTICA.4.000826
Optica, 4, 7, pp. 826-830, 2017-07-19

Research Article Vol. 4, No. 7 / July 2017 / Optica 826

optica

Producing and controlling half-cycle near-infrared electric-field transients

T. J. Hammond,[1,2,*] D. M. Villeneuve,[1] and P. B. Corkum[1]

[1]Joint Attosecond Science Laboratory, National Research Council and University of Ottawa, 100 Sussex Drive, Ottawa, Ontario K1A 0R6, Canada
[2]Department of Physics, University of Central Florida, Orlando, Florida 32816, USA
*Corresponding author: hammond.tj@gmail.com

Received 31 March 2017; revised 16 June 2017; accepted 16 June 2017 (Doc. ID 291749); published 19 July 2017

In a few-cycle laser pulse, the peak field strength depends on the carrier envelope phase. Concurrently, coherent control requires the measurement and manipulation of the spectral phase of a light pulse to influence a dynamical process that has multiple interfering pathways. Here, we exploit the interference of second harmonic generation and self-phase modulation in an 80 μm thick quartz plate due to a two-cycle pulse centered at 1.8 μm with peak intensity 3×10^{13} W/cm^2 to generate half-cycle electric field transients. In a monolithic step, we transform a measurement of the carrier envelope phase to the control over the pulse evolution with subcycle temporal accuracy. The high-intensity subcycle transient is scalable in pulse energy and will be useful for strong field physics and attosecond science: the ultrashort infrared pulse can generate isolated attosecond pulses from low bandgap semiconductor materials, and will be able to optically control currents on a subfemtosecond timescale.

OCIS codes: (190.4720) Optical nonlinearities of condensed matter; (320.5540) Pulse shaping; (320.7110) Ultrafast nonlinear optics; (320.6629) Supercontinuum generation.

https://doi.org/10.1364/OPTICA.4.000826

1. INTRODUCTION

The interference between quantum mechanically distinct pathways enables coherent control of chemistry [1], drives currents in solid state devices [2,3], and transforms mode-locked lasers into frequency combs [4,5]. Influenced by the latter, we self-phase modulate two-cycle 1.8 μm pulses in sub-100-μm-thick crystalline quartz to produce a spectrum that spans multiple octaves, while simultaneously exploiting non-phase-matched second harmonic generation to frequency up-convert the broadened spectrum.

A coherent supercontinuum spectrum without temporal chirp produces few-cycle pulses. The supercontinuum spectrum is typically generated through self-phase modulation in isotropic media, such as condensed matter [6,7], photonic crystal fiber [8,9], or noble gases [10,11]. In the extreme case of single and subcycle pulses, the complete control of the entire spectral phase becomes difficult [12]. The pulse is separated into several spectral branches, either rooted in a common multioctave spanning laser [13–15], or from separate lasers [12,16,17]. Each branch is temporally compressed, and all branches are coherently recombined. The resulting field requires not only the active stabilization of the phase of the seed laser pulse, but also careful dispersion management and subfemtosecond control of each spectral branch. In this paper, we propose and demonstrate a simplified method of generating a half-cycle transient field in the near infrared. Although there is less control over each step in the pulse compression process compared with previous techniques, our monolithic approach is considerably simpler to implement.

The nonlinear index of refraction depends only on the intensity (not the field), and is therefore independent of the carrier envelope phase (CEP). We use a thin quartz crystal—a material that can generate the second harmonic in parallel polarization to the fundamental field—to augment the bandwidth of the spectrum. The interference between the self-phase modulation and second harmonic generation depends on the CEP and leads to a pulse envelope reshaping, thereby introducing a strong CEP dependence in the supercontinuum. When operating in the anomalous dispersion regime, the newly created frequency components maintain the phase of the driving field and further compress the pulse. Using this ultra-broadband pulse restructuring, we synthesize intensity transients as short as half an optical cycle in a monolithic step while simultaneously measuring the absolute carrier envelope phase of the driving field. We also demonstrate that nonlinear pulse compression can passively stabilize the transmitted CEP, making electric field transients possible for low-repetition-rate, high-power lasers and attosecond science [18].

The phase of the second harmonic is determined by the CEP and quartz thickness and limits the independent control of the second harmonic phase relative to the fundamental. The spectral phase of the multioctave-spanning half-cycle transient also requires that the central frequency is in the anomalous dispersion regime, which limits the initial bandwidth of the pulse (for quartz, this is 1.3–3 μm). The relatively low nonlinear susceptibilities ($\chi^{(2)}$ and $\chi^{(3)}$) require that we operate at relatively high intensities, above 1×10^{13} W/cm^2.

2. METHODS

We generate ultrashort pulses centered at 1.8 μm from the idler of a CEP stable optical parametric amplifier (HE-TOPAS). To create the few-cycle pulses, we focus the 1 mJ, 70 fs duration idler into a hollow-core fiber with 1.1 Bar argon and compress to two cycles with 3 mm of fused silica; the output is 600 μJ and 11 fs duration [19]. We control the CEP with a pair of fused silica wedges placed either before or after the fiber.

We loosely focus (confocal parameter 10 cm) the few-cycle pulse onto an 80 μm thick monocrystalline quartz. A thin medium allows us to maintain one-dimensional propagation throughout the material. The spectrum of the few-cycle driving field broadens through self-phase modulation, where the light intensity controls the degree of self-phase modulation. The quartz is X cut with the polarization along the ordinary crystal direction to create the second harmonic. We combine self-phase modulation with second harmonic generation (taking place over the short coherence length of the material) to create the supercontinuum spectrum. The relative phase of the two pathways is sensitive to the CEP. We record the spectrum with either a visible or an infrared spectrometer.

To demonstrate that the CEP-dependent spectral modulation leads to a temporal modification, we measure the field transient with the petahertz (PHz) optical oscilloscope technique [20]. (The experimental setup is shown in Supplement 1.) We separate the fundamental field into two arms: the generating arm and the signal arm. In the generating arm, we use polarization gating (PG) to generate the isolated attosecond pulse, measured as a supercontinuum XUV spectrum with a two-dimensional spectrometer. The peak intensity is 1×10^{14} W/cm^2 incident on a krypton gas jet, backing pressure 6 Bar with a 250 μm diameter nozzle.

The signal arm, 10% power of the fundamental, is delayed by a nanometer resolution delay stage and focused onto the quartz sample with a 20 cm focal length mirror for a peak intensity up to 5×10^{13} W/cm^2. A 15 cm focal length mirror is on a micrometer resolution stage to control the divergence. The signal arm is further attenuated by a 3% reflection from glass, and is sent to a 30 cm focal length mirror to the gas jet. The relative intensity of the signal arm to the generating arm is estimated to be $I_s/I_g = 9 \times 10^{-4}$ with a relative angle of 20 mrad. The PHz optical oscilloscope records the deflection caused by the signal arm, $\sigma = dE/dt$, which is the derivative of the signal electric field. We measure the signal by following the peak of the XUV profile (at 25 ± 1 eV) as we delay the signal field relative to the generating arm. We digitally filter the signal with a filter bandwidth of 400 nm to 8 μm to remove XUV pointing drifts during acquisition; the field is calculated by integrating the resulting signal.

Further experimental setup details are given in Supplement 1.

3. RESULTS AND DISCUSSION

Because we observe little change in the infrared (the fundamental) portion of the spectrum, we first focus on the effect of the quartz on the visible (low-order harmonics) portion, shown in Fig. 1. We irradiate the quartz at low intensity, $I_{\text{peak}} = 1 \times 10^{13}$ W/cm^2, well below the damage threshold for quartz (greater than 4×10^{13} W/cm^2 for a two-cycle pulse centered at 1.8 μm). In Fig. 1(a), the interference fringes, which measure the relative CEP, arise from the second harmonic (generated within the quartz) interfering with the third harmonic that is generated in the hollow-core fiber (see Supplement 1) [21].

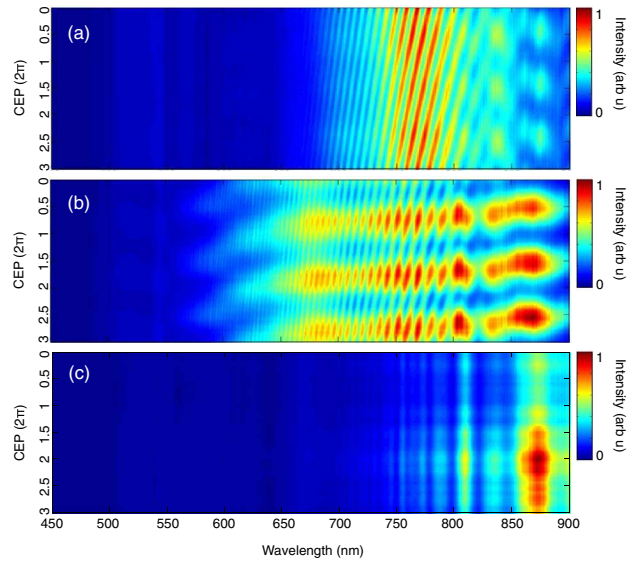

Fig. 1. Visible portion of the spectrum after quartz. (a) At low intensity, $I_{\text{peak}} = 1 \times 10^{13}$ W/cm^2, the spectral modulation shows an interference that is dependent on the CEP. (b) At moderate intensity, $I_{\text{peak}} = 3 \times 10^{13}$ W/cm^2, there is also an amplitude modulation due to the strong interference of the second harmonic and self-phase modulation. (c) Without the second harmonic, where the incident polarization is parallel to the optic axis, there is no second harmonic generated and no spectral modulation $I_{\text{peak}} = 3 \times 10^{13}$ W/cm^2.

At moderate intensities, $I_{\text{peak}} = 3 \times 10^{13}$ W/cm^2, there is an additional strong amplitude modulation, shown in Fig. 1(b). The amplitude modulation is a signature of the interference of the generated second harmonic, estimated to be approximately 2% in intensity of the fundamental, with the self-phase-modulated fundamental in parallel polarization (see Supplement 1). In this case, the relative phases of the fundamental and low-order harmonics depend on the CEP and cause amplitude modulation. This spectral amplitude gives additional information on the laser phase, enabling the measurement of the absolute value of the CEP [22].

To confirm the origin of the modulation, we rotate the quartz plate through 90°, such that the polarization is along the optic axis. This rotation eliminates the second harmonic, but keeps all other parameters constant. The spectrum becomes independent of the CEP, shown in Fig. 1(c). Thus, second harmonic generation in the quartz plate plays a vital role in both the broadband modulation of the spectrum in Fig. 1(b) and in the higher frequency spectral interference found in both Figs. 1(a) and 1(b).

We perform the temporal field measurement, the PHz optical oscilloscope, for different values of the CEP, obtaining the results shown in Fig. 2. The two traces have an estimated peak intensity incident on the quartz of $I_{\text{peak}} = 2.5 \times 10^{13}$ W/cm^2. We set the signal arm CEP $= 0$ such that we increase the spectral content, and we measure the dominant field transient to be as short as half an optical cycle, as shown in Fig. 2(a). When we change the signal arm CEP by π, we decrease the spectral content, and the field transient increases to approximately two cycles, as shown in Fig. 2(b). The square of the electric field is shown in Fig. 2(c). We can see that for the case of CEP $= 0$, the measured square of

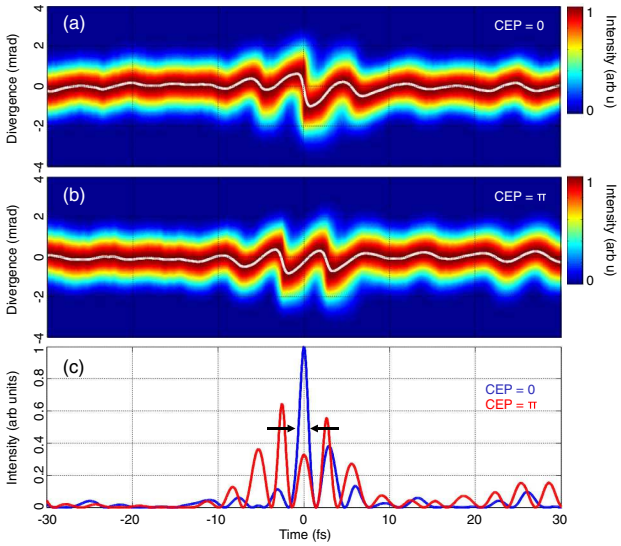

Fig. 2. PHz optical oscilloscope traces for two values of the CEP differing by π. We measure a pulse of (a) one half-cycle in duration, or (b) more than one cycle in duration. (c) The square of the measured field shows the pulse duration. For the half-cycle case, the FWHM is 1.3 fs (arrows).

the field yields a half-cycle pulse, where the full width at half maximum (FWHM) duration is 1.3 fs.

Figure 3(a) shows our calculation of the intensity envelope as a function of CEP, for an incident peak intensity of $I_{\text{peak}} = 2 \times 10^{13}$ W/cm^2. We simulate this case in one dimension (1D) within the quartz using the Forward Maxwell's Equation, shown to be robust for few-cycle pulses [23]. We use the second harmonic $d_{\text{eff}} = 0.3$ pm/V [24] and nonlinear index of refraction of $n_2 = 3.2 \times 10^{-16}$ cm^2/W for our 80 μm thick quartz sample, along with an estimate of the nonlinear spectral dependence [25]. We do not account for spatiotemporal coupling and propagation after the quartz in this simulation. Changing the fundamental CEP changes the phase of the second harmonic, modifying the intensity envelope; the interference between the second harmonic and the fundamental modifies the pulse envelope and changes the pulse duration. At certain values of the CEP, the destructive interference of the second harmonic with the fundamental suppresses the field before and after the main portion of the pulse, thereby shortening the pulse duration. We then take the intensity

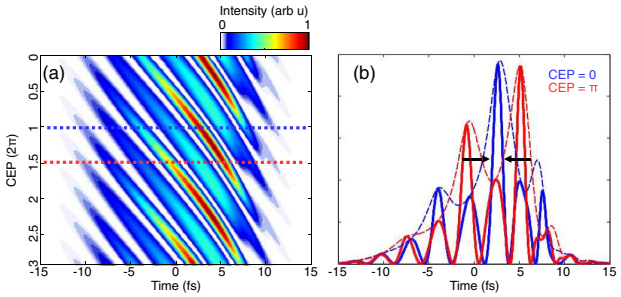

Fig. 3. Simulation of the pulse intensity. (a) The intensity (the field square) modulates as a function of CEP due to the second harmonic. (b) Two selected values of the CEP, 0 and π (blue and red, respectively), show the change in pulse shape (envelope dash lines, field solid lines). For CEP = 0, the envelope has a FWHM pulse duration of 2.3 fs, while the square of the field duration (black arrows) is 1.2 fs.

profile at two CEP values, shown in Fig. 3(b). For CEP = 0 (blue), there is one dominating half-cycle, where the FWHM pulse duration (envelope, dashed) is 2.3 fs, while the square of the field (thick line) has a FWHM pulse duration of 1.2 fs. The pulse duration increases to 7 fs when the CEP changes by π (red).

We increase the incident intensity on the quartz plate, with the polarization perpendicular to the crystal axis to generate a second harmonic. With $I_{\text{peak}} = 4 \times 10^{13}$ W/cm^2 (near the damage threshold), we expect little energy deposited to the sample [26]. We now find that the interference fringes are not linear as a function of the CEP. The measured visible spectrum is shown in Fig. 4(a), while a 1D calculation is shown in Fig. 4(b). The spectral modulation now has a nonlinear dependence on the input CEP. Over certain values of the CEP, the spectral modulation becomes less dependent on the driving field CEP (shown by the black line in the insets). This spectral modulation, which represents a measurement of the pulse phase, signifies that after propagating through the quartz the resulting phase is nonlinearly correlated to the driving field CEP.

Figure 4(c) shows the calculated electric field as a function of CEP. The steep slope of the peak of the electric field near 7 fs results from a nonlinear phase delay of the temporally distorted and compressed pulse due to pulse self-steepening. The modification of the field leads to less CEP phase change of the emerging pulse than on the input pulse: the CEP of the propagating pulse does not depend linearly on the CEP of the input. This nonlinear temporal compression leads to self-stabilization and reduces the energy to phase coupling found in CEP measurements [27]. This stabilization can benefit strong field physics, where high peak intensities are obtained with low-repetition-rate systems that are difficult to stabilize [28].

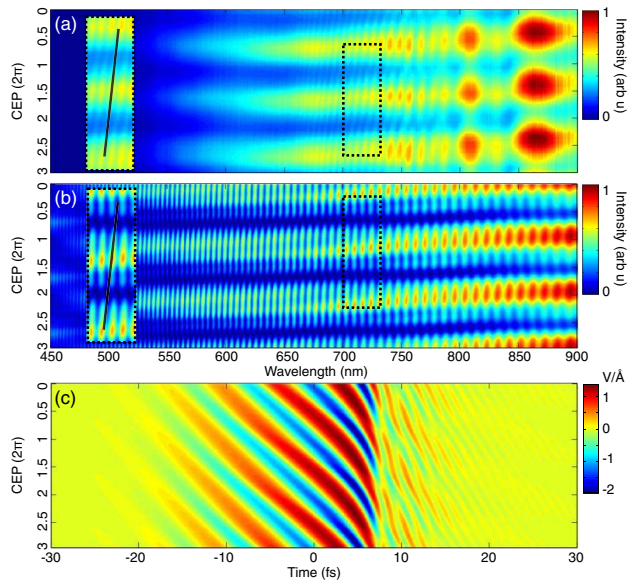

Fig. 4. At high intensity, $I_{\text{peak}} = 4 \times 10^{13}$ W/cm^2, the spectral modulation becomes nonlinear as a function of CEP; (a) experiment and (b) theory. Insets: zoom-in of spectrum from 700 to 730 nm (black dashed box); black line is a guide for the CEP measurement at large spectral amplitude. When the visible spectral amplitude is maximum, the modulation becomes less dependent on the CEP. (c) The calculated field (scale V/Å) as a function of CEP has a nonlinear phase delay; the nonlinear temporal shift leads to a nonlinear CEP dependence.

4. CONCLUSIONS

Field synthesis can be performed in a monolithic manner. We exploit the interplay between different orders of nonlinearities within quartz for field synthesis while we simultaneously measure the CEP of the synthesized pulse. In our experiment, generating subcycle field transients is aided by the low group-delay-dispersion of the low-order harmonics, enabling us to lock the phases across a newly generated spectrum spanning multiple octaves. However, we could also use materials with higher susceptibilities that can more efficiently generate the second harmonic in parallel polarization to the fundamental, and that have a higher nonlinear index of refraction. These materials may allow for thinner, less dispersive optics [29], and could broaden the range of driving laser frequencies where monolithic field synthesis can be used. Furthermore, we can incorporate multipass configurations, such as the geometries used for thin-disk lasers [30], where the multiple passes through the material increase the bandwidth [31] while dispersion-compensating mirrors redirect the beam. This relatively simple setup would allow for the generation of half-cycle transients directly from an amplifier, while the thin optic requires little dispersion compensation and, in principle, should incur little loss. It may even be possible to structure the material itself, so that alternating layers of the optic can take advantage of the higher nonlinear susceptibilities, and other layers can compensate for the dispersion using different materials.

Reproducible behavior of multiphoton processes with few-cycle pulses requires that we control the CEP [32]. In a few-cycle pulse, changing the field within the envelope changes the peak field amplitude [33], which then modifies the multiphoton ionization rate of atoms and time of electron–ion recollision [34]. In attosecond pulse generation, this dependence changes the generated XUV flux, spectrum, and spectral phase [35]. We expect that this half-cycle transient pulse will be able to generate isolated attosecond pulses from gases in the XUV to hundreds of electronvolts. We also expect to generate isolated attosecond pulses condensed matter [36], where the infrared central wavelength can drive currents from low-bandgap semiconductor materials.

Funding. Defense Advanced Research Projects Agency (DARPA) (W31P4Q1310017)); Air Force Office of Scientific Research (AFOSR) (FA9550-15-1-0037, FA9550-16-1-0109); Army Research Office (ARO) (W911NF-, 14-1-0383); Natural Sciences and Engineering Research Council of Canada (NSERC); Canada Foundation for Innovation (CFI); Ontario Research Fund (ORF).

Acknowledgment. We thank Kyung Taec Kim for useful discussions, as well as the support of Dr. Andrei Naumov and the technical assistance of Dave Crane and Bert Avery.

See Supplement 1 for supporting content.

REFERENCES

1. P. Brumer and M. Shapiro, "Control of unimolecular reactions using coherent light," Chem. Phys. Lett. **126**, 541–546 (1986).
2. E. Dupont, P. Corkum, H. C. Lu, M. Buchanan, and Z. R. Wasilewski, "Phase-controlled current in semiconductors," Phys. Rev. Lett. **74**, 3596–3599 (1995).
3. A. Haché, Y. Kostoulas, R. Atanasov, J. Hughes, J. Sipe, and H. van Driel, "Observation of coherently controlled photocurrent in unbiased, bulk GaAs," Phys. Rev. Lett. **78**, 306–309 (1997).
4. D. J. Jones, S. A. Diddams, J. K. Ranka, A. Stentz, R. S. Windeler, J. L. Hall, and S. T. Cundiff, "Carrier-envelope phase control of femtosecond mode-locked lasers and direct optical frequency synthesis," Science **288**, 635–639 (2000).
5. A. Apolonski, A. Poppe, G. Tempea, C. Spielmann, T. Udem, R. Holzwarth, T. W. Hänsch, and F. Krausz, "Controlling the phase evolution of few-cycle light pulses," Phys. Rev. Lett. **85**, 740–743 (2000).
6. C.-H. Lu, Y.-J. Tsou, H.-Y. Chen, B.-H. Chen, Y.-C. Cheng, S.-D. Yang, M.-C. Chen, C.-C. Hsu, and A. H. Kung, "Generation of intense supercontinuum in condensed media," Optica **1**, 400–406 (2014).
7. V. Shumakova, P. Malevich, S. Ališauskas, A. Voronin, A. Zheltikov, D. Faccio, D. Kartashov, A. Baltuška, and A. Pugžlys, "Multi-millijoule few-cycle mid-infrared pulses through nonlinear self-compression in bulk," Nat. Commun. **7**, 12877 (2016).
8. B. Schenkel, R. Paschotta, and U. Keller, "Pulse compression with supercontinuum generation in microstructure fibers," J. Opt. Soc. Am. B **22**, 687–693 (2005).
9. T. Balciunas, C. Fourcade-Dutin, G. Fan, T. Witting, A. Voronin, A. Zheltikov, F. Gerome, G. Paulus, A. Baltuska, and F. Benabid, "A strong-field driver in the single-cycle regime based on self-compression in a kagome fibre," Nat. Commun. **6**, 6117 (2015).
10. M. Nisoli, S. Stagira, S. D. Silvestri, O. Svelto, S. Sartania, Z. Cheng, M. Lenzner, C. Spielmann, and F. Krausz, "A novel-high energy pulse compression system: generation of multigigawatt sub-5-fs pulses," Appl. Phys. B **65**, 189–196 (1997).
11. B. E. Schmidt, P. Béjot, M. Giguère, A. D. Shiner, C. TralleroHerrero, É. Bisson, J. Kasparian, J.-P. Wolf, D. M. Villeneuve, J.-C. Kieffer, P. B. Corkum, and F. Légaré, "Compression of 1.8 mm laser pulses to sub two optical cycles with bulk material," Appl. Phys. Lett. **96**, 121109 (2010).
12. S. H. Chia, G. Cirmi, S. Fang, G. M. Rossi, O. D. Muecke, and F. X. Kaertner, "Two-octave-spanning dispersion controlled precision optics for sub-optical-cycle waveform synthesizers," Optica **1**, 315–322 (2014).
13. G. Krauss, S. Lohss, T. Hanke, A. Sell, S. Eggert, R. Huber, and A. Leitenstorfer, "Synthesis of a single cycle of light with compact erbium-doped fibre technology," Nat. Photonics **4**, 33–36 (2010).
14. A. Wirth, M. T. Hassan, I. Grguraš, J. Gagnon, A. Moulet, T. T. Luu, S. Pabst, R. Santra, Z. A. Alahmed, A. M. Azzeer, V. S. Yakovlev, V. Pervak, F. Krausz, and E. Goulielmakis, "Synthesized light transients," Science **334**, 195–200 (2011).
15. M. T. Hassan, T. T. Luu, A. Moulet, O. Raskazovskaya, P. Zhokhov, M. Garg, N. Karpowicz, A. M. Zheltikov, V. Pervak, F. Krausz, and E. Goulielmakis, "Optical attosecond pulses and tracking the nonlinear response of bound electrons," Nature **530**, 66–70 (2016).
16. S. Huang, G. Cirmi, J. Moses, K. Hong, S. Bhardwaj, J. Birge, L. Chen, E. Li, B. J. Eggleton, G. Cerullo, and F. X. Kaertner, "High-energy pulse synthesis with sub-cycle waveform control for strong-field physics," Nat. Photonics **5**, 475–479 (2011).
17. J. A. Cox, W. P. Putnam, A. Sell, A. Leitenstorfer, and F. X. Kaertner, "Pulse synthesis in the single-cycle regime from independent mode-locked lasers using attosecond precision feedback," Opt. Lett. **37**, 3579–3581 (2012).
18. Z. Chang, P. B. Corkum, and S. R. Leone, "Attosecond optics and technology: progress to date and future prospects," J. Opt. Soc. Am. B **33**, 1081–1097 (2016).
19. C. Zhang, G. Vampa, D. M. Villeneuve, and P. B. Corkum, "Attosecond lighthouse driven by sub-two-cycle, 1.8 mm laser pulses," J. Phys. B **48**, 061001 (2015).
20. K. T. Kim, C. Zhang, A. D. Shiner, B. E. Schmidt, F. Légaré, D. M. Villeneuve, and P. B. Corkum, "Petahertz optical oscilloscope," Nat. Photonics **7**, 958–962 (2013).
21. T. Tritschler, O. D. Muecke, M. Wegener, U. Morgner, and F. X. Kaertner, "Evidence for third-harmonic generation in disguise of second-harmonic generation in extreme nonlinear optics," Phys. Rev. Lett. **90**, 217404 (2003).
22. T. Wittmann, B. Horvath, W. Helml, M. G. Schátzel, X. Gu, A. L. Cavalieri, G. G. Paulus, and R. Kienberger, "Singleshot carrier–envelope phase measurement of few-cycle laser pulses," Nat. Phys. **5**, 357–362 (2009).

23. A. Husakou and J. Hermann, "Supercontinuum generation of higher-order solitons by fission in photonic crystal fibers," Phys. Rev. Lett. **87**, 203901 (2001).
24. D. Roberts, "Simplified characterization of uniaxial and biaxial nonlinear optical crystals: a plea for standardization of nomenclature and conventions," IEEE J. Quantum Electron. **28**, 2057–2074 (1992).
25. W. Ettoumi, Y. Petit, J. Kasparian, and J.-P. Wolf, "Generalized Miller formulae," Opt. Express **18**, 6613–6620 (2010).
26. A. Sommer, E. M. Bothschafter, S. A. Sato, C. Jakubeit, T. Latka, O. Razskazovskaya, H. Fattahi, M. Jobst, W. Schweinberger, V. Shirvanyan, V. S. Yakovlev, R. Kienberger, K. Yabana, N. Karpowicz, M. Schultze, and F. Krausz, "Attosecond nonlinear polarization and light–matter energy transfer in solids," Nature **534**, 86–90 (2016).
27. C. Li, E. Moon, H. Wang, H. Mashiko, C. M. Nakamura, J. Tackett, and Z. Chang, "Determining the phase-energy coupling coefficient in carrier-envelope phase measurements," Opt. Lett. **32**, 796–798 (2007).
28. E. Cunningham, Y. Wu, and Z. Chang, "Carrier-envelopephase control of a 10 Hz, 25 TW laser for high-flux extreme ultraviolet quasi-continuum generation," Appl. Phys. Lett. **107**, 201108 (2015).
29. D. Haertle, M. Jazbinsek, G. Montemazzani, and P. Günter, "Nonlinear optical coefficients and phase-matching conditions in $Sn_2P_2S_6$," Opt. Express **13**, 3765–3776 (2005).
30. A. Giesen and J. Speiser, "Fifteen years of work on thin-disk lasers: results and scaling laws," IEEE J. Sel. Top. Quantum Electron. **13**, 598–609 (2007).
31. P. He, Y. Liu, K. Zhao, H. Teng, X. He, P. Huang, H. Huang, S. Zhong, Y. Jiang, S. Fang, X. Hou, and Z. Wei, "High-efficiency supercontinuum generation in solid thin plates at 0.1 TW level," Opt. Lett. **42**, 474–477 (2017).
32. R. Kienberger, E. Goulielmakis, M. Uiberacker, A. Baltuska, V. Yakovlev, F. Bammer, A. Scrinzi, T. Westerwalbesloh, U. Kleineberg, U. Heinzmann, M. Drescher, and F. Krausz, "Atomic transient recorder," Nature **427**, 817–821 (2004).
33. F. Krausz and M. Ivanov, "Attosecond physics," Rev. Mod. Phys. **81**, 163–234 (2009).
34. E. Goulielmakis, M. Schultze, M. Hofstetter, V. S. Yakovlev, J. Gagnon, M. Uiberacker, A. L. Aquila, E. M. Gullikson, D. T. Attwood, R. K. F. Krausz, and U. Kleineberg, "Single-cycle nonlinear optics," Science **320**, 1614–1617 (2008).
35. T. J. Hammond, G. G. Brown, K. T. Kim, D. Villeneuve, and P. B. Corkum, "Attosecond pulses measured from the attosecond lighthouse," Nat. Photonics **10**, 171–175 (2016).
36. M. Garg, M. Zhan, T. T. Luu, H. Lakhotia, T. Klostermann, A. Guggenmos, and E. Goulielmakis, "Multi-petahertz electronic metrology," Nature **538**, 359–363 (2016).